JACS
JOURNAL OF THE AMERICAN CHEMICAL SOCIETY
Communication
pubs.acs.org/JACS

Graphite-Conjugated Pyrazines as Molecularly Tunable Heterogeneous Electrocatalysts

Tomohiro Fukushima,[§] Walter Drisdell,[†] Junko Yano,[†,‡] and Yogesh Surendranath*[,§]

[§]Department of Chemistry, Massachusetts Institute of Technology, Cambridge, Massachusetts 02139, United States
[†]Joint Center for Artificial Photosynthesis and [‡]Physical Biosciences Division, Lawrence Berkeley National Laboratory, Berkeley, California 94720, United States

Supporting Information

ABSTRACT: Condensation of *ortho*-phenylenediamine derivatives with *ortho*-quinone moieties at edge planes of graphitic carbon generates graphite-conjugated pyrazines (GCPs) that are active for oxygen reduction electrocatalysis in alkaline aqueous electrolyte. Catalytic rates of oxygen reduction are positively correlated with the electrophilicity of the active site pyrazine unit and can be tuned by over 70-fold by appending electron-withdrawing substituents to the phenylenediamine precursors. Discrete molecular analogs containing pyrazine moieties display no activity above background under identical conditions. This simple bottom up method for constructing molecularly well-defined active sites on ubiquitous graphitic solids enables the rational design of tunable heterogeneous catalysts.

The interconversion of electrical and chemical energy requires the coupling of electron transfer with substrate bond rearrangement. This interconversion can be achieved at surface-exposed active sites of heterogeneous electrocatalysts[1] or via redox mediation facilitated by a homogeneous molecular electrocatalyst.[2] Molecular electrocatalysts yield readily to synthetic alteration of their redox properties, permitting systematic tuning of catalyst activity and selectivity.[3] Similar control is difficult to achieve with heterogeneous electrocatalysts because they typically exhibit a distribution of active site geometries and local electronic structures,[4] which are recalcitrant to molecular-level synthetic modification. However, heterogeneous electrocatalysts typically exhibit greater durability and are more readily integrated into functional energy conversion devices such as fuel cells and electrolyzers. In principle, the attractive features of heterogeneous and molecular catalysts can be combined if robust methods are developed for constructing well-defined, tunable active sites on the surfaces of conductive solids.

Typically, molecular electrocatalysts are heterogenized by introducing an inert tether between the active site and the electrode surface.[5] However, there exists a paucity[6] of surface connection chemistries that are both robust and well-defined. For example, thiol-based self-assembled monolayers allow for a high degree of surface uniformity,[7] but exhibit a limited range of electrochemical stability.[8] In contrast, harsher ligation methods involving electrogenerated radicals[9] forge robust covalent linkages with carbon surfaces but are prone to form ill-defined polymeric multilayers and are incompatible with sensitive molecular functionality.[9] Additionally, these methods inherently impose a tunneling barrier for electron transfer, limiting the rate of electron flux to the active site.

Herein, we introduce an orthogonal strategy for constructing molecularly well-defined surface active sites that exploits the native surface chemistry of graphitic carbon, obviating the need for an exogenous linker. We show that condensation of *ortho*-phenylenediamines with *ortho*-quinone moieties present on the edge planes of graphitic carbons[10,11] generates graphite-conjugated pyrazine (GCP) moieties that are active for oxygen reduction catalysis in alkaline aqueous electrolytes. GCPs constitute a new class of well-defined heterogeneous catalysts in which the active site reactivity can be systematically tuned at the molecular level by modifying the diamine precursor (Scheme 1).

Scheme 1. Condensation of *ortho*-Phenylenediamine Derivatives with *ortho*-Quinone Edge Sites of Graphene Sheets To Generate GCPs

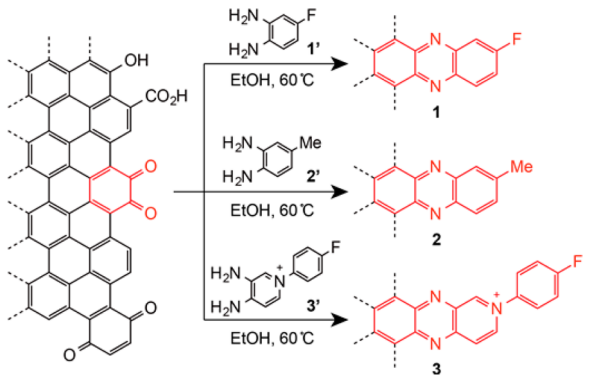

To facilitate systematic studies of oxygen reduction catalysis, GCPs were synthesized on glassy carbon (GC) electrodes, which contain graphitic domains with a high edge to basal plane ratio.[10b,c] To clean the GC surface and increase the population of surface quinone groups, electrodes were subjected to brief anodic treatment following literature methods.[12] We then treated the anodized GC electrodes with the requisite phenylenediamine precursor in ethanol at 60 °C for 12 h, after which, the electrodes

Received: June 29, 2015

DOI: 10.1021/jacs.5b06737
J. Am. Chem. Soc. XXXX, XXX, XXX−XXX

were rinsed with copious amounts of pure ethanol, water, and 0.1 M $HClO_4$. By employing differentially substituted diamines, three distinct GCP catalysts, **1**−**3**, were obtained (Scheme 1).

To characterize the surface species generated by this synthetic protocol, we examined **1**−**3** via X-ray photoelectron spectroscopy (XPS). Data for **1** are shown in Figure 1a (XPS data for **2** and **3** are shown in Figure S1, and fitting parameters are summarized in Table S1). Upon functionalization of the GC electrode with **1**′, a pronounced peak is observed in the N 1s XPS spectrum at 398.9 eV binding energy that is absent in the native electrode (Figure S2). This peak position is in line with that expected for pyridinic nitrogen moieties on N-containing carbons.[13] In addition, we observed a sharp F 1s peak at 687.0 eV binding energy (Figure 1a inset), and XPS spectra reveal an N/F ratio of ∼2, in line with the atomic composition of **1**′. These same spectral features are also observed in the N 1s spectra for **2** and **3**, with an additional peak observed at 401.7 eV for **3**, diagnostic of the pyridinium nitrogen (Figure S1).[13] Together the data indicate that *ortho*-phenylenediamines chemically ligate to glassy carbon surfaces.

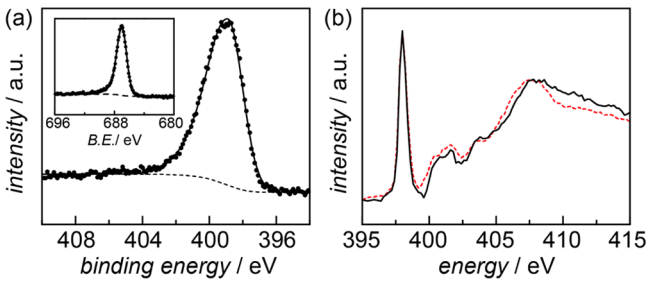

Figure 1. (a) High-resolution N 1s and F 1s (inset) XPS spectra of **1**. (b) N K-edge XANES of **1**′-treated high surface area carbon (black solid line) and phenazine (red dashed line).

To gain further insight into the local bonding environment of nitrogen centers,[14] we probed **1**′-treated high surface area graphitic carbon, Monarch 1300, by nitrogen K-edge X-ray absorption near edge structure (XANES) spectroscopy (Figure 1b, black). Combustion analysis of this high surface area variant of **1** reveals an increase in N content from 0.1 to 1.3 mass % (Table S2), consistent with incorporation of **1**′ into the high surface area carbon. The XANES spectra of the modified carbon display a sharp feature at 398.0 eV assigned to the 1s−π^* transition. This transition is followed by a series of broad features spanning 407 to 409 eV which are assigned to 1s−σ^* transitions. An excellent match is observed between the spectrum of phenazine (Figure 1b, red dashed line) and high surface area carbon treated with **1**′ (Figure 1b, solid line). The observed spectral features are distinct from those observed for free aryl amines in **1**′ (Figure S3) or imidazole nitrogens, which display a pre-edge feature at 401 eV,[15] 2 eV blueshifted relative to that observed for the Monarch 1300-modified GCP. Thus, the good spectral agreement between phenazine and the modified carbon suggests a negligible population of free amines or surface imidazoles. The latter, which could arise from condensation of *ortho*-phenylenediamines with surface carboxylic acids, requires strong acid catalysis and high temperatures[15] and is thus disfavored under these mild conditions. Together, these data establish that the synthetic protocol in Scheme 1 selectively generates surface pyrazinic units and that this chemistry is generally applicable to both low surface area glassy carbons and high surface area graphitic carbons.

Conveniently, surface pyrazine units display reversible redox features in aqueous electrolytes that are absent in untreated electrodes (Figure S4).[11] Slow scan cyclic voltammograms of **1**−**3** (Figure 2, black) in N_2-saturated 0.1 M KOH reveal reversible

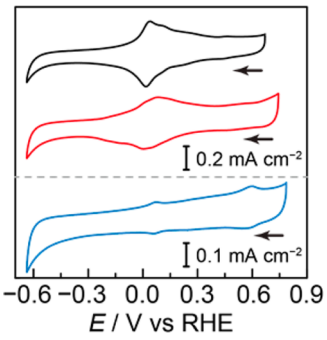

Figure 2. Cyclic voltammograms (5 mV/s scan rate) of **1** (black), **2** (red), and **3** (blue) recorded in N_2-saturated 0.1 M KOH electrolyte.

waves with formal potentials of $E_{1/2}$ = 0.01, 0.05, and 0.48 V (all potentials are reported versus the reversible hydrogen electrode, RHE), respectively. **3** also exhibits a second redox wave at 0.07 V, attributed to subsequent reduction of the pyrazine core. The peak currents scale linearly with scan rate (Figure S5), and small peak-to-peak separations were observed, indicating that the redox features result from a surface-bound rather than diffusing species. Importantly, substitution of the diamine precursor has a dramatic influence on the redox potential, with the strongly electron-withdrawing pyridinium unit in **3** imposing a ∼0.5 V shift in the first redox potential. In all cases, the redox waves are broad, displaying a peak width at half height of >200 mV, significantly greater than the 90.6/n mV value expected for ideal noninteracting surface-bound molecular centers.[16] We attribute the broadness of these redox features to lateral electrostatic interactions[17] on the surface between proximate pyrazine units as well as interactions between pyrazine units and charged surface oxides.

Integration of these redox waves provides an estimate of the surface site density of electroactive pyrazines. Accounting for the surface roughness of the anodized GC electrode (see Figures S6, S7, and Table S3) and assuming two electrons transferred per pyrazine unit, we calculated site densities of ∼0.25 nmol cm^{-2} for **1** and **2**, and 14 pmol cm^{-2} for **3**. The values obtained for **1** and **2** are comparable to the coverages observed for self-assembled monolayers on Au electrodes,[18] indicating that the surface population of pyrazines in **1** and **2** is relatively high, whereas the surface population of **3** is ∼20-fold lower. The relatively low site density observed for **3** may be due to electrostatic repulsion of pyridinium units on the surface inhibiting a high degree of incorporation.

GCPs are active for oxygen reduction catalysis as prepared without any thermal annealing. Figure 3a shows linear sweep voltammograms of an unmodified GC rotating disk electrode (dotted black line) and **1** (solid black line). Whereas the unmodified GC electrode shows a catalytic onset potential of ∼0.6 V, **1** displays catalytic onset at 0.75 V and displays 18-fold higher current at 0.6 V. The differential substitution pattern of **2** and **3** gives rise to a systematic change in catalytic activity; the electron-donating methyl group in **2** leads to an ∼18 mV shift to higher overpotential at 1 mA cm^{-2} current density, whereas the electron-withdrawing pyridinium moiety in **3** leads to an ∼24 mV shift to lower overpotential at the same current density. Owing to

DOI: 10.1021/jacs.5b06737
J. Am. Chem. Soc. XXXX, XXX, XXX−XXX

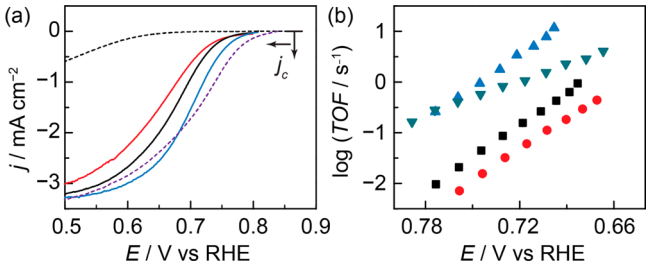

Figure 3. (a) Linear sweep voltammograms (5 mV/s scan rate) of **1** (black), **2** (red), **3** (blue), 3′-treated Monarch 1300 (dotted purple) and unmodified GC (dotted black) recorded in O_2-saturated 0.1 M KOH electrolyte. Data were recorded at 2000 rpm, and current densities are normalized to the geometric electrode area. (b) Tafel plots of per site activity vs applied potential for **1** (black), **2** (red), **3** (blue), and polycrystalline Ag (green).

a higher surface area, films of 3′-treated Monarch 1300 on GC disk electrodes (see SI for details of film preparation) exhibit a ~ 19 mV positive shift relative to **3** at the same current density. Importantly, exhaustive efforts to remove trace metal ion impurities from the KOH electrolyte via pre-electrolysis or chelation[18] resulted in no change in catalytic activity for the modified carbons (Figure S8), indicating that catalysis emerges from the surface pyrazine moiety itself rather than adsorbed metal ion impurities from the electrolyte. Together, these results establish that GCPs display oxygen reduction activity that can be incrementally tuned via derivatization of the phenylenediamine precursor.

To probe catalytic efficiency and mechanism in greater detail, we collected steady-state measurements of the activation-controlled current density for oxygen reduction as a function of applied potential. Independently prepared electrodes exhibit very similar activities (Figure S9), highlighting the reproducibility of this system. The activation controlled currents were obtained from Koutechky–Levich (K-L) plots for larger overpotentials (representative K-L plots are shown in Figure S10). Activation controlled currents were then normalized to the integrated charge passed to reduce the electroactive surface pyrazine in the absence of O_2 (see above), thereby generating turnover frequency (TOF) values in electrons transferred per pyrazine site per second.

Tafel plots of the log of the TOF vs the applied potential are shown in Figure 3b and reveal that the rate of oxygen reduction is highly sensitive to the substitution pattern of the GCP catalyst. Whereas methyl-substituted GCP, **2**, (Figure 3b, red) displays a TOF of 0.12 ± 0.01 s^{-1} at 0.7 V, fluoro-substituted GCP, **1**, is nearly 3-fold more active (Figure 3b, black) at the same potential with a TOF of 0.35 ± 0.04 s^{-1}. Interestingly, **3** displays a TOF value of 8.6 ± 0.2 s^{-1} at the same potential (Figure 3b, blue), which is more than one order of magnitude greater than the TOF values of **1**, and similar to the TOF values observed for polycrystalline Ag (Figure 3b, green) on a per site basis (see SI for calculation of Ag site density). To the best of our knowledge, this is the first report of a per-site TOF for a metal-free N-containing carbon. Interestingly, **1**–**3** all display similar Tafel slopes of 60 ± 5 mV/decade, indicating that they all proceed through a reversible one electron transfer step followed by rate-limiting chemistry.[19] These results establish that heterogeneous oxygen reduction catalysis can be tuned with molecular-level specificity using this simple surface condensation chemistry.

To probe the selectivity of **1**–**3** for four-electron reduction of O_2 to water, we conducted rotating ring-disk electrode voltammetry (Figure S11). The Faradaic efficiency for water production was found to be ~77% at 0.7 V and rises to ~94% at 0 V for 3′-treated high surface area carbon. Additionally, long-term potentiostatic electrolysis of **1** reveals only 7% decay in catalytic activity over 12 h (Figure S12). Based on the total charge passed over this time period, this corresponds to a lower limit TON of ~8000. Over the same time period **3** slowly deactivates to ~50% of its initial activity (Figure S12) with similar Faradaic efficiency for water production (Figure S13). We attribute the activity decay to base-catalyzed hydrolysis of the pyridinium moiety.[20] However, following initial decay, **3** then exhibits sustained catalytic activity comparable to **1** (Figure S12), highlighting the robustness of the pyrazine linkage under harsh electrocatalytic conditions.

GCPs display significantly greater oxygen reduction activity than homogeneous molecular analogs. For this comparison, we chose carboxy-substituted molecular pyrazine derivatives due to their enhanced water solubility. Thus, to provide a fair comparison, we prepared 4-carboxy-substituted GCP, **4**, which bears the same substitution pattern. Cyclic voltammograms of the molecular analogs, pyrazine (Figure 4a, red), quinoxaline-6-carboxylic acid (Figure 4a, green), and dibenzo[*a*,*c*]phenazine-2-carboxylic acid (Figure 4a, blue) display reversible waves in the absence of O_2. The former two molecules exhibit peak currents that scale linearly with the square root of the scan rate, diagnostic of a diffusing species (Figures S14 and S15), whereas the wave for the latter arises from both adsorbed and diffusing species (Figure S16). As the number of fused rings increases across this series, the formal reduction potential shifts positively by ~0.3 V to a value comparable to the main peak observed for 4-carboxy substituted GCP, **4** (Figure 4a, brown). Interestingly, oxygen reduction reaction catalytic current for all of the molecular analogs is actually suppressed relative to the background activity of the freshly polished GC electrode, suggesting that these molecules deactivate the electrode toward oxygen reduction catalysis. Indeed, increasing the concentration of quinoxaline-6-carboxylic acid only serves to suppress catalytic activity further (Figure S17). In contrast, **4** displays catalytic onset ~100 mV more positive than the GC background. The unique performance of the GCP may arise from surface conjugated species with more positive potentials than that of discrete molecules (Figure 4a) or

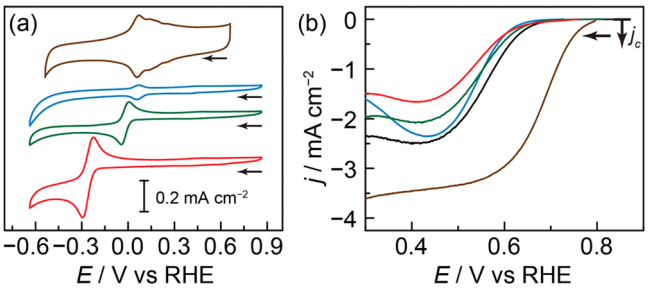

Figure 4. (a) Cyclic voltammograms of pyrazine (red), quinoxaline-6-carboxylic acid (green), dibenzo[*a*,*c*]phenazine-2-carboxylic acid (blue) and **4** (brown) recorded in N_2-saturated 0.1 M KOH. (b) Linear sweep voltammograms of a freshly polished GC disk electrode rotated at 2000 rpm and recorded in O_2-saturated 0.1 M KOH electrolyte containing 5 mM pyrazine (red), 5 mM quinoxaline-6-carboxylic acid (green), 1 mM dibenzo[*a*,*c*]phenazine-2-carboxylic acid (blue), and no molecular catalyst (black). Liner sweep voltammogram of **4** (brown) recorded at 2000 rpm in O_2-saturated 0.1 M KOH. All data recorded at 5 mV/s scan rate.

DOI: 10.1021/jacs.5b06737
J. Am. Chem. Soc. XXXX, XXX, XXX–XXX

to an intrinsic role of extended conjugation in lowering the barrier for electron transfer and O_2 activation.[21] Together, these data highlight that GCPs can display potent multielectron reactivity, which is absent in discrete molecular analogs.

In conclusion, we have demonstrated that simple *ortho*-phenylenediamine derivatives can be selectively ligated to *ortho*-quinone functionalities found ubiquitously on edge planes of graphitic carbons. As prepared, the resulting GCP units exhibit high activity for oxygen reduction catalysis. Owing to the molecular nature of the surface active site, the overpotential for oxygen reduction catalysis can be systemically decreased by increasing the electrophilicity of the pyrazine core, reaching per site turnover frequencies rivaling metallic polycrystalline silver. Interestingly, GCPs display higher catalytic activity than discrete homogeneous molecular analogs bearing identical functionality. Given their facile preparation and the wide array of accessible phenylenediamine derivatives, GCPs are poised to serve as a powerful platform for constructing molecularly well-defined, tunable heterogeneous catalysts.

■ ASSOCIATED CONTENT

Supporting Information

The Supporting Information is available free of charge on the ACS Publications website at DOI: 10.1021/jacs.5b06737.

Experimental details, synthesis and characterization data for molecular precursors, XPS, XANES, elemental analysis of high surface area carbons, and additional electrochemical characterization data (PDF)

■ AUTHOR INFORMATION

Corresponding Author

*yogi@mit.edu

Notes

The authors declare no competing financial interest.

■ ACKNOWLEDGMENTS

T.F. thanks Y. Inamoto, K. Kawasumi, and M. Risch for fruitful discussions. This work was supported by a JSPS postdoctoral fellowship for research abroad for T.F. This work was also supported by the U.S. Department of Energy, Office of Science, Office of Basic Energy Sciences, under award number DE-SC0014176 and by the MIT Department of Chemistry through junior faculty funds for Y.S. XAS experiments were supported by the Joint Center for Artificial Photosynthesis, a DOE Energy Innovation Hub, supported through the Office of Science of the U.S. Department of Energy under award no. DE-SC0004993 and performed at the Advanced Light Source (BL 6.3.1), Berkeley, under contract DE-AC02-05CH11231.

■ REFERENCES

(1) (a) Trasatti, S. *J. Electroanal. Chem. Interfacial Electrochem.* **1972**, *39*, 163−184. (b) Surendranath, Y.; Nocera, D. G. *Prog. Inorg. Chem.* **2011**, *57*, 505−560.

(2) (a) Savéant, J.-M. *Chem. Rev.* **2008**, *108*, 2348−2378. (b) DuBois, M. R.; DuBois, D. L. *Chem. Soc. Rev.* **2009**, *38*, 62−72. (c) Benson, E. E.; Kubiak, C. P.; Sathrum, A. J.; Smieja, J. M. *Chem. Soc. Rev.* **2009**, *38*, 89−99.

(3) (a) Hawecker, J.; Lehn, J.-M.; Ziessel, R. *J. Chem. Soc., Chem. Commun.* **1984**, 328−330. (b) Chang, C. J.; Loh, Z.-H.; Shi, C.; Anson, F. C.; Nocera, D. G. *J. Am. Chem. Soc.* **2004**, *126*, 10013−10020. (c) Concepcion, J. J.; Jurss, J. W.; Templeton, J. L.; Meyer, T. J. *J. Am. Chem. Soc.* **2008**, *130*, 16462−16463. (d) McNamara, W. R.; Han, Z.; Yin, C.-J.; Brennessel, W. W.; Holland, P. L.; Eisenberg, R. *Proc. Natl. Acad. Sci. U. S. A.* **2012**, *109*, 15594−15599. (e) Carver, C. T.; Matson, B. D.; Mayer, J. M. *J. Am. Chem. Soc.* **2012**, *134*, 5444−5447. (f) Sampson, M. D.; Nguyen, A. D.; Grice, K. A.; Moore, C. E.; Rheingold, A. L.; Kubiak, C. P. *J. Am. Chem. Soc.* **2014**, *136*, 5460−5471.

(4) (a) Jaramillo, T. F.; Jørgensen, K. P.; Bonde, J.; Nielsen, J. H.; Horch, S.; Chorkendorff, I. *Science* **2007**, *317*, 100−102. (b) Li, C. W.; Ciston, J.; Kanan, M. W. *Nature* **2014**, *508*, 504−507.

(5) (a) Collman, J. P.; Devaraj, N. K.; Decréau, R. A.; Yang, Y.; Yan, Y.-L.; Ebina, W.; Eberspacher, T. A.; Chidsey, C. E. D. *Science* **2007**, *315*, 1565−1568. (b) Le Goff, A.; Artero, V.; Jousselme, B.; Tran, P. D.; Guillet, N.; Métayé, R.; Fihri, A.; Palacin, S.; Fontecave, M. *Science* **2009**, *326*, 1384−1387. (c) McCrory, C. C. L.; Devadoss, A.; Ottenwaelder, X.; Lowe, R. D.; Stack, T. D. P.; Chidsey, C. E. D. *J. Am. Chem. Soc.* **2011**, *133*, 3696−3699. (d) Yao, S. A.; Ruther, R. E.; Zhang, L.; Franking, R. A.; Hamers, R. J.; Berry, J. F. *J. Am. Chem. Soc.* **2012**, *134*, 15632−15635.

(6) (a) Devadoss, A.; Chidsey, C. E. D. *J. Am. Chem. Soc.* **2007**, *129*, 5370−5371. (b) Ruther, R. E.; Rigsby, M. L.; Gerken, J. B.; Hogendoorn, S. R.; Landis, E. C.; Stahl, S. S.; Hamers, R. J. *J. Am. Chem. Soc.* **2011**, *133*, 5692−5694.

(7) Love, J. C.; Estroff, L. A.; Kriebel, J. K.; Nuzzo, R. G.; Whitesides, G. M. *Chem. Rev.* **2005**, *105*, 1103−1169.

(8) Beulen, M. W. J.; Kastenberg, M. I.; van Veggel, F. C. J. M.; Reinhoudt, D. N. *Langmuir* **1998**, *14*, 7463−7467.

(9) (a) Pinson, J.; Podvorica, F. *Chem. Soc. Rev.* **2005**, *34*, 429−439. (b) Mahouche-Chergui, S.; Gam-Derouich, S.; Mangeney, C.; Chehimi, M. M. *Chem. Soc. Rev.* **2011**, *40*, 4143−4166. (c) Sheridan, M. V.; Lam, K.; Geiger, W. E. *J. Am. Chem. Soc.* **2013**, *135*, 2939−2942.

(10) (a) Boehm, H.-P.; Diehl, E.; Heck, W.; Sapok, R. *Angew. Chem., Int. Ed. Engl.* **1964**, *3*, 669−677. (b) McCreery, R. L. *Chem. Rev.* **2008**, *108*, 2646−2687. (c) Wildgoose, G. G.; Abimana, P.; Compton, R. G. *J. Mater. Chem.* **2009**, *19*, 4875−4886.

(11) Thorogood, C. A.; Wildgoose, G. G.; Crossley, A.; Jacobs, R. M. J.; Jones, J. H.; Compton, R. G. *Chem. Mater.* **2007**, *19*, 4964−4974.

(12) Engstrom, R. C. *Anal. Chem.* **1982**, *54*, 2310−2314.

(13) (a) Arrigo, R.; Hävecker, M.; Wrabetz, S.; Blume, R.; Lerch, M.; McGregor, J.; Parrott, E. P. J.; Zeitler, J. A.; Gladden, L. F.; Knop-Gericke, R.; Schlögl, R.; Su, D. S. *J. Am. Chem. Soc.* **2010**, *132*, 9616−9630. (b) Li, Q.; Noffke, B. W.; Wang, Y.; Menezes; Peters, D. G.; Raghavachari, K.; Li, L.-S. *J. Am. Chem. Soc.* **2014**, *136*, 3358−3361.

(14) Mitra-Kirtley, S.; Mullins, O. C.; Van Elp, J.; George, S. J.; Chen, J.; Cramer, S. P. *J. Am. Chem. Soc.* **1993**, *115*, 252−258.

(15) Fitton, A. O.; Smalley, R. K. *Practical Heterocyclic Chemistry*; Academic Press, Inc.: London, 1968.

(16) Bard, A. J.; Faulkner, L. R. *Electrochemical Methods: Fundamentals and Applications*, 2nd ed.; Wiley-VCH: New York, 2001; p 591.

(17) Chidsey, C. E. D.; Bertozzi, C. R.; Putvinski, T. M.; Mujsce, A. M. *J. Am. Chem. Soc.* **1990**, *112*, 4301−4306.

(18) Wuttig, A.; Surendranath, Y. *ACS Catal.* **2015**, *5*, 4479−4484.

(19) Gileadi, E. *Physical Electrochemistry: Fundamentals, Techniques and Applications*; Wiley-VCH: New York.

(20) Vanderwal, C. D. *J. Org. Chem.* **2011**, *76*, 9555−9567.

(21) Li, Q.; Zhang, S.; Dai, L.; Li, L.-S. *J. Am. Chem. Soc.* **2012**, *134*, 18932−18935.

DOI: 10.1021/jacs.5b06737
J. Am. Chem. Soc. XXXX, XXX, XXX−XXX